F08

Proceedings of the 5th International Conference on Inverse Problems in Engineering: Theory and Practice, Cambridge, UK, 11-15th July 2005

STABILIZATION OF ILL-POSED PROBLEMS THROUGH THE DATA SPACE: HEAT CONDUCTION THEORY

J.I. FRANKEL
Mechanical, Aerospace and Biomedical Engineering Department, University of Tennessee, Knoxville, TN, USA, 37996-2210
e-mail: vfrankel@earthlink.net

Abstract- Transient surface heat fluxes are often interpreted from surface temperature measurements (calorimetry). Unfortunately, inherent time differentiation of the surface temperature data is either explicitly performed by the user or implicitly performed by the numerical method. Increasing the sample density exacerbates the problem even further. In this paper, we present compelling evidence suggesting that the surface heat flux can be accurately recovered using inaccurate heating/cooling rate sensors. To demonstrate this hypothesis, this paper develops analytic inversions to the one- and two-dimensional integral equations governing the relationship between surface temperature and heat flux in the half space. The resulting integral expressions display directions of stability from which the surface heat flux can be recovered. That is, measuring surface temperature leads to an unstable direction for heat flux recovery while measuring the surface heating/cooling rate leads to a stable direction for heat flux recovery. Numerical results supporting this claim are presented for the transient, one-dimensional, linear heat equation. Using heating/cooling rate data, stability and accuracy increase as the sample density increases which is unlike the situation involving temperature measurements.

1. INTRODUCTION

The precise measurement of temperature and heat flux are basic quantities of interest in heat transfer. These quantities have been traditionally sought and numerous sensors have been developed capable of producing accurate results over various conditions, applications and thermal ranges. High temperature, heat fluxes and heating/cooling rates are of practical concern owing to their appearance in aerospace, defense and nuclear applications. The mathematical development described in this paper is often used for estimating the penetrating heat flux into an opaque solid as indicated in Figure 1 (arcjet for emulating planetary, reentry conditions), or for investigating thin film heat flux gauges.

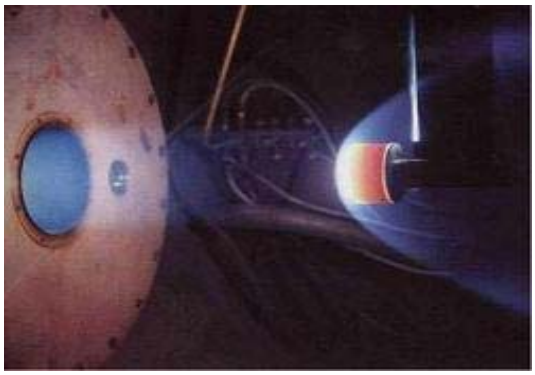

Figure 1: Arcjet stagnation model in Martian atmosphere [1].

Applications can be subdivided into real-time requirements or post-processing analysis. Diagnostics and evaluation applications collect data that can be analyzed at a later time in order to evaluate thermophysical properties or deduce surface heat fluxes from measured temperatures. In contrast, health monitoring and control may require real-time analysis from which immediate decisions can be made. Aerospace applications [1] that will greatly benefit from new sensor developments include: (i) advanced in-flight sensor systems for atmospheric entry maneuvers, (ii) hypersonic aerothermodynamics, (iii) arcjet operation/testing of TPS materials for various atmosphere, (iv) real-time health management in aerothermal structures, (v) surface heat flux determination for estimating dissociation degree based on embedded or surface mounted sensors, and thermophysical property evaluation.

Several basic requirements for developing the accurate capture and interpretation of data consistently appear. In particular, the need exists for developing methods that permit the quantitative evaluation of local errors, and new real-time intrusive and nonintrusive measurement techniques for application in highly hostile environments. Often probes cannot be attached at the desired location due to hostile environments. Embedded sensors are used to deduce or project to the location of interest. This often leads to ill-posed problems in which error amplification will most certainly dominate [2,3]. Inverse problems [4] are termed "ill-posed" in the sense of Hadamard since a small perturbation in the "input" can produce randomly large variations in the "output". The word "input" here is related to the state variable or solution. This situation is unlike the analysis of "direct" problems, in that, a small perturbation in the input produces a small perturbation in the output. It is interesting to note that differentiation of data represents the most fundamental ill-posed problem [3]. Numerical differentiation of noisy data is known to be ill-posed in the sense of Hadamard since small perturbations in the function can lead to large variations in the derivative. This can quickly be understood by noting that the absolute error associated with a forward difference approximation to $f'_\epsilon(x)$ in the presence of noisy data results in the error bound $f'_\epsilon < O(h) + 2\delta/h$ where δ is the maximum absolute error, i.e., $|f - f_i| < \delta$, and h is the conventional step size. Therefore, for $\delta > 0$, as $h \to 0$ the resulting error bound blows up. Thus, $h \to 0$ cannot be performed in an arbitrary manner.

In transient heat transfer situations, it is well known that the order of the differential equation (in time) gives insight into the best form of data to be collected. However, this important mathematical fact is often put aside in lieu of using traditional sensors based on temperature and heat flux. For example, the transient heat equation expressed in temperature is first order in time. Thus, if data were presented in heating/cooling rate terms (dT/dt), the severity of the ill-posed nature is basically reduced [5]. Changing the data space can effectively remove the ill-posedness. Direct differentiation of data by coarse grid regularization or other such methods may require the removal of physically important data. Several methods involving some form of Tikhonov regularization have also been developed.

Zeroth-order sensors have been used for over 50 years. It is critical to note that the development of analytic methods for resolving inverse problems has been brought about based on the available sensors. These analytical methods are complicated and do not assure accuracy in the output. We propose to invert the process, that is, develop sensors based on the analysis that will provide stable and accurate predictions even if the sensor is inaccurate.

2. MATHEMATICAL FORMULATIONS

In this section, two examples are mathematically formulated illustrating the advantages associated with developing new, rate-based thermal sensors. The first formulation involves the classical one-dimensional, half-space heat conduction problem whereby a surface measurement is used to determine the spatially uniform, time varying, penetrating surface heat flux. The second formulation presents the two-dimensional extension of the one-dimensional, half-space formulation. It is again shown that similar sensor requirements are needed for assuring stability and accuracy in the prediction of the spatially and temporally varying penetrating surface heat flux. This section illustrates that it is mathematically possible to identify an appropriate sensor by apriori analysis.

2.1 One-dimensional, half-space heat conduction

Kulish and Lage [6] have investigated several transient, linear, half-space heat transfer problems and developed novel integral relationships between the temperature and heat flux. This local relationship (not solution) is quite useful in the half-space investigations considered by Kulish and Lage. Their integral relationships permit two distinct interpretations. The first is direct and stable while the second is inverse and normally unstable (depending on the data space). The first involves the specification of the local heat flux from which the local temperature is determined. This statement only requires the implementation of integration. The second involves the specification of temperature from which the local heat flux is reconstructed. This situation leads to a Volterra integral equation of the first kind. If discrete, noisy temperature data are specified then this formulation is unstable.

In [6], the heat flux is analytically provided leading to a relatively simple numerical procedure for obtaining the corresponding temperature. Frankel *et al.* [5] have noted that this defines a stable numerical direction. However, determining the heat flux from discrete, noisy temperature data leads to an unstable numerical prediction. That is, the prediction noticeably worsens as either the noise level or sample density increases. Regularization methods are normally implemented in order to arrive at an acceptable prediction. Determining the optimal regularization parameter is crucial and often difficult to achieve. The quality of the prediction is closely connected to optimal regularization parameter.

To circumvent this unfavorable characteristic, Frankel *et al.* [5] have analyzed the concept of using an alternative data space. This idea involves using higher-time derivative measurements involving the temperature and heat flux. Frankel *et al.* [5] have developed several theoretical concepts for measuring the proposed hierarchical system involving dT/dt, dq''/dt and d^2T/dt^2. The move toward real-time analysis may benefit from the development of such higher-time derivative measurement techniques.

The linear, heat conduction equation under consideration is given by [5]

$$\frac{\partial T}{\partial t}(x,t) = \alpha \frac{\partial^2 T}{\partial x^2}(x,t), \quad x \in (-\infty, \infty), \quad t \geq 0, \tag{1a}$$

where α is the thermal diffusivity. Equation (1a) is subject to the initial condition $T(x,0) = T_o$. Following the development of [6], the integral relationship between the temperature $T(x,t)$ and heat flux $q''(x,t) = -k\frac{\partial T}{\partial x}(x,t)$ is

$$T(x,t) = T_o + \lambda \int_0^t q''(x,t_o) K(t,t_o) dt_o, \quad x \in (-\infty, \infty), t \geq 0, \tag{1b}$$

where the convolution kernel $K(t,t_o)$ is given as

$$K(t,t_o) = \frac{1}{\sqrt{t-t_o}}, \quad t > t_o, \tag{1c}$$

with $\lambda = 1/\sqrt{\pi k \rho c_p}$, k is the thermal conductivity, ρ is the density, and c_p is the heat capacity. At the surface ($x = 0$), eqn. (1b) reduces to [5]

$$T(0,t) = T_o + \lambda \int_0^t q''(0,t_o) K(t,t_o) dt_o, \quad t \geq 0. \tag{1d}$$

It should be noted that the Green's function solution [5,7] leads to identical result at the boundary $x = 0$. Equation (1d) is merely the classical Abel integral equation having known inversion properties [5,8]. Frankel *et al.* [5] developed a hierarchical inversion sequence of the Abel equation to provide insight into devising a proper sensor sequence for stable predictions. That is, an Abel inversion [5] indicates a stable data space from which data should be collected. For simplicity but without loss of generality, the boundary relationship at $x = 0$ is the focus of the present analysis though any position x can be equally analyzed using the approach taken here. Also, without loss of generality, let $T_o = 0^o C$. The Abel inversion process is standard [5,8]. However, in light of the novel two-dimensional development to be shown in the next subsection, some intermediate steps are described. We begin by operating on eqn.(1d)(after replacing t by the dummy variable u) with $\frac{1}{\sqrt{t-u}}$ and integrating over the domain of interest to arrive at

$$\int_0^t \frac{T(0,u)}{\sqrt{t-u}} du = \lambda \int_0^t \int_0^u q''(0,t_o) \frac{K(u,t_o)}{\sqrt{t-u}} dt_o du, \quad t \geq 0. \tag{2a}$$

Upon carefully interchanging orders of integration on the triangle, we obtain

$$\int_0^t \frac{T(0,u)}{\sqrt{t-u}} du = \lambda \pi \int_0^t q''(0,t_o) dt_o, \quad t \geq 0, \tag{2b}$$

since

$$\int_{t_o}^t \frac{K(u,t_o)}{\sqrt{t-u}} du = \pi. \tag{2c}$$

Next, we integrate the left-hand side of eqn.(2b) by parts and then differentiate eqn. (2b) with respect to time t, using Leibnitz's rule, to obtain the well-known result

$$q''(0,t) = \frac{1}{\lambda \pi} \int_0^t \frac{\partial T(0,t_o)}{\partial t_o} K(t,t_o) dt_o, \quad t \geq 0, \tag{2d}$$

where we have returned to the original dummy variable of integration. Equation (2d) is a working inversion formula for the penetrating surface heat flux $q''(0,t)$ when provided $\partial T(0,t)/\partial t$. This is in stark contrast to eqn. (1d) which is a weakly-singular Volterra integral equation of the first kind for the surface heat flux when provided $T(0,t)$ data. It is well known that first-kind Volterra equation [8] are mildly ill posed. Since experimental data are inexact, its real-time use in numerical schemes must be viewed

with some care. That is, real-time use requires using the interpreted value without consideration to its error band. This, of course, is incorrect but convenient. Differentiation of such data is well known to be ill-posed in the classical sense. It is not normally recommend to use these data exactly since they place too much emphasis on their inexact value. However, by changing the data space, it will be demonstrated that measurements with a high degree of error can produce more accurate and stable results than measurements having a low degree of error. The choice of the data space must thus be considered. These remarks involve the direct measurement or interpretation of thermal "rate" quantities.

2.2 **Two-dimensional, half-space heat conduction**

In this subsection, we extend the one-dimensional analysis previously described to two spatial dimensions as schematically shown in Figure 2. A novel development is offered that has a rigorous theoretical foundation. The inverted heat equation identifies the optimal sensor for assuring the predictive accuracy and stability of the surface heat flux based on a surface measurement. Consider the two-dimensional, constant property heat equation

$$\frac{\partial^2 T}{\partial x^2}(x,z,t) + \frac{\partial^2 T}{\partial z^2}(x,z,t) = \frac{1}{\alpha}\frac{\partial T}{\partial t}(x,z,t), \quad x \in (-\infty,\infty), \quad z \in (0,\infty), \quad t > 0, \tag{3}$$

subject to the initial condition $T(x,z,0) = T_o = 0^oC$.

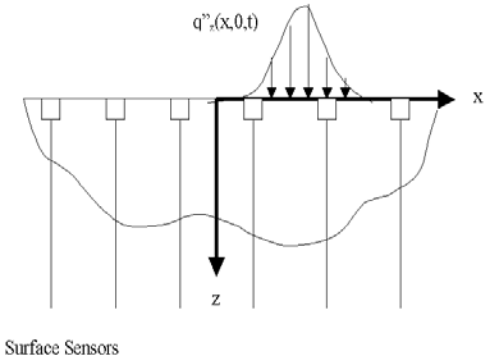

Figure 2: Two-dimensional, half-space with spatially and temporally varying heat flux with surface mounted sensors.

With the aid of the Green's functions method [7] or other integral transform methods, the equivalent integral relationship between the surface temperature and penetrating surface heat flux at $z = 0$ is

$$T(x,0,t) = \frac{1}{2\pi k}\int_0^t \int_{-\infty}^{\infty} K_1(x,t;x_o,t_o) q_z''(x_o,0,t_o) dx_o dt_o, \quad x \in (-\infty,\infty), \quad t \geq 0, \tag{4a}$$

where the kernel $K_1(x,t;x_o,t_o)$ is

$$K_1(x,t;x_o,t_o) = \frac{e^{-\frac{(x-x_o)^2}{4\alpha(t-t_o)}}}{t-t_o}, \quad (x,x_o) \in (-\infty,\infty), \quad t \geq t_o, \tag{4b}$$

and the heat fluxes in the x, z directions are defined as

$$q_x''(x,z,t) = -k\frac{\partial T}{\partial x}(x,z,t), \tag{4c}$$

$$q_z''(x,z,t) = -k\frac{\partial T}{\partial z}(x,z,t), \tag{4d}$$

respectively. It should be noted that if $q_z''(x,0,t) \to q_z''(t)$ then eqn. (4a) reduces to eqn. (1d) since it can be shown that

$$\int_{-\infty}^{\infty} e^{-\frac{(x-x_o)^2}{4\alpha(t-t_o)}} dx_o = 2\sqrt{\alpha\pi(t-t_o)}. \tag{5}$$

As with the one-dimensional case previously described, if the surface temperature $T(x,0,t)$ is prescribed then a first kind (ill-posed) Volterra-Fredholm equation for the heat flux is mathematically obtained. As expected, this will lead to immediate numerical problems if provided noisy, discrete surface temperature information. Note that if one is provided the heat flux, $q_z''(x,0,t)$ then a mere integral definition is produced leading to most likely accurate temperature predictions (assuming that the bias has been removed from the data). Equation (4a) appears representative of a Cauchy-type integral equation unlike eqn.(1b) which is representative of an Abel equation with known inversion properties [5,8] .

However, from theoretical viewpoint, we can operate on eqn.(4a) with the Abel kernel $1/\sqrt{t-u}$ (after replacing t by u in eqn.(4a)) and integrate over the time domain of interest to produce

$$\int_0^t \frac{T(x,0,u)}{\sqrt{t-u}}du = \frac{1}{2\pi k}\int_0^t\int_0^u\int_{-\infty}^{\infty} q_z''(x_o,0,t_o)\frac{e^{-\frac{(x-x_o)^2}{4\alpha(u-t_o)}}}{\sqrt{t-u}(u-t_o)}dx_o dt_o du, \quad x\in(-\infty,\infty), \quad t\geq 0. \quad (6)$$

Carefully, interchanging orders involving the temporal variables, we find

$$\int_0^t \frac{T(x,0,u)}{\sqrt{t-u}}du = \frac{1}{2\pi k}\int_0^t\int_{-\infty}^{\infty} q_z''(x_o,0,t_o)\frac{M(x,t;x_o,t_o)}{\sqrt{t-t_o}}dx_o dt_o, \quad x\in(-\infty,\infty), \quad t\geq 0, \qquad (7a)$$

since

$$\int_{t_o}^t \frac{e^{-\frac{(x-x_o)^2}{4\alpha(u-t_o)}}}{\sqrt{t-u}(u-t_o)}du = \frac{M(x,t;x_o,t_o)}{\sqrt{t-t_o}}, \qquad (7b)$$

and where the kernel, $M(x,t;x_o,t_o)$ is now given as

$$M(x,t;x_o,t_o) = e^{-\frac{(x-x_o)^2}{8\alpha(t-t_o)}}K_0\big(\frac{(x-x_o)^2}{8\alpha(t-t_o)}\big), \quad x_o\neq x, \qquad (7c)$$

where $K_o(v)$ is the modified Bessel function of the second kind of order zero [9] which contains a logarithmic (integrable) singularity at $v=0$. Again, note that both u and t_o are dummy variables of integration. Weak or integrable singularities are well studied and are not considered as an obstacle in the analysis. It should be noted that (i) $M(x,t;x_o,t_o)$ contains a logarithmic singularity for $t_o\neq t$, $x\rightleftharpoons x_o$, and (ii) $\lim_{t_o\to t}\frac{M(x,t;x_o,t_o)}{\sqrt{t-t_o}}\to 0$, $x_o\neq x$.

At this juncture, it should be observed that eqn.(7a) reduces to the one-dimensional case if $q_z''(x,0,t)\to q_z''(t)$, $T(x,0,t)\to T(0,t)$ shown in eqn.(2b) since

$$\int_{-\infty}^{\infty} M(x,t;x_o,t_o)dx_o = 2\sqrt{\alpha(t-t_o)}\pi^{\frac{3}{2}}. \qquad (8)$$

As with the one-dimensional development, we integrate the left-hand side of eqn. (7a) by parts but now, for convenience, we additionally add and subtract the indicated integral on the right-hand side to obtain

$$\begin{aligned} 2\int_0^t \sqrt{t-t_o}\frac{\partial T}{\partial t_o}(x,0,t_o)dt_o &= \frac{1}{2\pi k}\int_0^t\int_{-\infty}^{\infty} q_z''(x_o,0,t_o)\frac{M(x,t;x_o,t_o)}{\sqrt{t-t_o}}dx_o dt_o \\ &\pm\frac{1}{2\pi k}\int_0^t\int_{-\infty}^{\infty} q_z''(x,0,t_o)\frac{M(x,t;x_o,t_o)}{\sqrt{t-t_o}}dx_o dt_o, \quad x\in(-\infty,\infty), \quad t\geq 0, \end{aligned} \qquad (9a)$$

or upon regrouping

$$\begin{aligned} 2\int_0^t \sqrt{t-t_o}\frac{\partial T}{\partial t_o}(x,0,t_o)dt_o &= \frac{1}{2\pi k}\int_0^t\int_{-\infty}^{\infty} [q_z''(x_o,0,t_o)-q_z''(x,0,t_o)]\frac{M(x,t;x_o,t_o)}{\sqrt{t-t_o}}dx_o dt_o \\ &+\frac{1}{2\pi k}\int_0^t \frac{q_z''(x,0,t_o)}{\sqrt{t-t_o}}\int_{-\infty}^{\infty} M(x,t;x_o,t_o)dx_o dt_o, \quad x\in(-\infty,\infty), \quad t\geq 0, \end{aligned} \qquad (9b)$$

or upon using eqn. (8), we find

$$\begin{aligned} 2\int_0^t \sqrt{t-t_o}\frac{\partial T}{\partial t_o}(x,0,t_o)dt_o &= \frac{1}{2\pi k}\int_0^t\int_{-\infty}^{\infty} [q_z''(x_o,0,t_o)-q_z''(x,0,t_o)]\frac{M(x,t;x_o,t_o)}{\sqrt{t-t_o}}dx_o dt_o \\ &+\frac{\sqrt{\pi\alpha}}{k}\int_0^t q_z''(x,0,t_o)dt_o, \quad x\in(-\infty,\infty), \quad t\geq 0. \end{aligned} \qquad (9c)$$

Finally, we differentiate eqn. (9c) with the aid of Leibnitz's rule to obtain

$$q_z''(x,0,t) = \frac{1}{\lambda\pi}\int_0^t \frac{\partial T}{\partial t_o}(x,0,t_o)\frac{dt_o}{\sqrt{t-t_o}}$$

$$-\frac{1}{2\pi\sqrt{\alpha\pi}}\frac{\partial}{\partial t}\int_0^t\int_{-\infty}^{\infty}[q_z''(x_o,0,t_o)-q_z''(x,0,t_o)]\frac{M(x,t;x_o,t_o)}{\sqrt{t-t_o}}dx_o dt_o, \quad x\in(-\infty,\infty), \quad t\geq 0. \tag{10}$$

Equation (10) is merely one possible integral formulation that will be numerically investigated. Equation (10) is enlightening and suggestive though practically speaking other forms are better suited for actual numerical implementation. It is evident that as $q_z''(x,0,t)\rightarrow q_z''(t)$, $T(x,0,t)\rightarrow T(0,t)$ then eqn.(2a) is recovered. The time derivative located outside of the double integral is not carried through at this juncture. Equation (10) reveals that the measurement of the heating/cooling rate, $\frac{\partial T}{\partial t}(x,0,t)$ yields a stable, time stepping method for arriving at the heat flux distribution along all x and $t\geq 0$. At each sequential time step forward, the entire surface heat flux distribution, $q_z''(x,0,t)$ normal to the surface is obtained from eqn. (10). With $q_z''(x,0,t)$ determined, eqns (4a) and (4c) are used for determining the heat flux, $q_x''(x,0,t)$, if desired. This portion of the study is analytic in nature and does not address issues associated with optimal sensors placement nor acceptable sensor noise levels. These issues will be addressed in a future study.

3. NUMERICAL RESULTS

This section presents numerical results for the one-dimensional problem previously formulated. To demonstrate several key issues, consider the often encountered heat flux of the Gaussian form [10]

$$q''(0,t) = q_s''(t) = q_o'' e^{-(\frac{t-b}{\sigma})^2}, \quad t\geq 0, \tag{11}$$

where q_o'' is the maximum heat flux value acquired at $t=b$. The physical meanings for the parameters b and σ are self evident. For the present study, inexact, discrete data for the surface temperature $\{T_{s,i}\}_{i=1}^M$ and surface heating/cooling rate $\{\frac{dT_{s,i}}{dt}\}_{i=1}^M$ are provided. Here, M represents the number of measured data. Though not necessary, exact initial conditions are imposed at $t=0$ owing to their availability. Again, for demonstration purposes, the analysis and numerical results consider the surface at $x=0$. This example focuses on comparing two, discrete data forms (temperature, T_s and heating/cooling rate, dT_s/dt) and their abilities to recover the surface heat flux as the noise levels and sampling rates are varied.

Numerically "exact" temperature data are generated by discretizing eqn.(1d) using $q_s''(t)$ as defined in eqn.(11). Numerous numerical methods [8] are available for implementation. For this study, a product trapezoidal rule [8] is implemented for obtaining the discrete "exact" values of $T_s(t_i)$. A simple forward finite difference method is used to then develop the "exact" heating/cooling rate data set $\{dT_s(t_i)/dt\}_{i=0}^M$ based on these values. The noisy data sets are developed based on

$$T_{s,i} = T_s(t_i) + \|T_s(t)\|_\infty \epsilon_1 Random_{1,i}[-1,1], \tag{12a}$$

$$\frac{dT_{s,i}}{dt} = \frac{dT_s}{dt}(t_i) + \|\frac{dT_s}{dt}(t)\|_\infty \epsilon_2 Random_{2,i}[-1,1], \quad i=1,2,...,M, \tag{12b}$$

where $T_s(t_i)=T(0,t_i)$, $\|\Psi\|_\infty = max_{t\epsilon[0,t_{max}]}|\Psi(t)|$ is the infinity norm of the function $\Psi(t)$, ϵ_k, $k=1,2$ are noise levels while $Random_{k,i}$ are randomly drawn numbers from a uniform distribution in the interval $[-1,1]$ such that the mean error for each data set is zero.

Figure 3 ($M=3000$) displays both the numerically "exact" solution and noisy data sets for the surface temperature $T_s(t)$ and heating/cooling rate dT_s/dt when $\epsilon_1=0.0125$, $\epsilon_2=0.1$. Additionally, it is assumed that $b=2.5\times 10^{-4}sec.$, $\sigma=5\times 10^{-5}sec.$, $q_o''=75000W/cm^2$, $k=52W/(mK)$, and $\rho c_p = 1.73\times 10^6 J/(m^3\ K)$. For this plot, the discrete time, t_i is defined using $t_i=i\Delta t$, $i=1,2,...,M$, where $\Delta t = t_{max}/M$ and $t_{max}=0.001sec.$ Throughout this presentation, solid lines represent numerically "exact" results. In these figures, open circles are associated with temperature data while open triangles are associated with heating/cooling rate data.

The relative simplicity of eqn.(1d) permits use of a Newton-Cotes right-hand rectangular rule for resolving the first kind integral equation [8] for predicting $q''(0,t)=q_s''(t)$ based on surface temperature data. This simple numerical approach can be modified at a later time if required. This implementation is also used for discretizing eqn.(2d) for predicting the surface heat flux $q''(0,t)=q_s''(t)$ based on heating/cooling rate data. The product integration method is applied only to the singular kernel contributions

while a conventional Newton-Cotes rectangular method is implemented elsewhere. Another annoying feature of ill conditioned (or ill posed) problems is observable as the approximation is refined or the sampling rate is increased. In direct or forward problems, normally better results are generated as the approximation is refined. This is not the case with ill-posed problems. As the approximation is refined, the error in the output may begin to increase. Thus, an optimal prediction occurs at some unknown juncture.

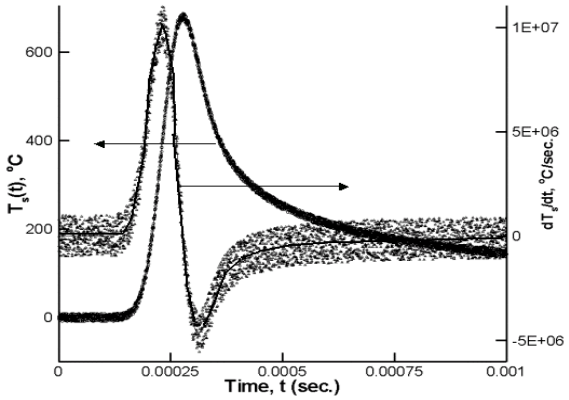

Figure 3: Temperature, $T_s(t)$ (solid line-exact, open circle-noisy data, $\epsilon_1 = 0.0125$, eqn.(12a)) and heating/cooling rate, dT_s/dt (solid line-exact, open triangle-noisy data, $\epsilon_2 = 0.1$,eqn. (12b)) used for simulation when $M = 3000$.

Figures 4 and 5 present predictions for the surface heat flux based on the data presented in Figure 3 ($M = 3000$). Figure 4 displays a) the exact heat flux given in eqn.(11) by the solid line, b) the numerically predicted heat flux using eqn. (1d) when $\epsilon_1 = 0$ by the dashed line, and c) the numerically predicted heat flux using eqn. (1d) when $\epsilon_1 = 0.0125$ by the open circles. The numerical method nearly replicates the exact heat flux when the discrete data contain no induced errors ($\epsilon_1 = 0$). Figure 5 presents a corresponding set of results to that of Figure 4 with the exception that eqn. (2d) is solved using heating/cooling rate data prescribed in Figure 3. Figure 5 displays a) the exact heat flux given in eqn.(11) by the solid line, b) the numerically predicted heat flux using eqn.(2d) when $\epsilon_2 = 0$ by the dashed line, and c) the numerically predicted heat flux using eqn.(2d) when $\epsilon_2 = 0.1$ by the open triangles. Again, as expected, the numerical procedure nearly emulates the exact solution when the discrete data contains zero noise. The noisy data set associated with the heating/cooling rate data produces a more accurate heat flux prediction than that developed by the corresponding temperature data set containing less error. As expected, error amplification is not graphically observed when using $\{dT_{s,i}/dt\}_{i=1}^{M}$.

In order to consider the concept of stability and accuracy based on the data space some norms require introduction. The root-mean-square of the output error is defined as

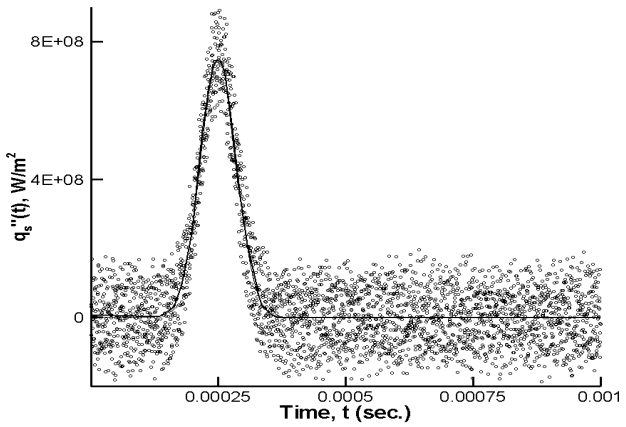

Figure 4: Predicted heat fluxes, $q_s''(t)$ using temperature data a) solid line-exact, eqn.(11); b) dashed line-errorless data predictions, $\epsilon_1 = 0$, eqn.(1d); and c) open circles-noisy data predictions, $\epsilon_1 = 0.0125$, eqn.(1d) when $M = 3000$.

.

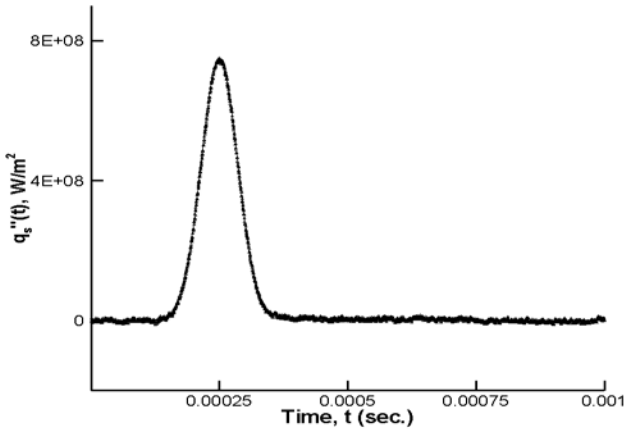

Figure 5: Predicted heat fluxes, $q_s''(t)$ using heating/cooling rate data a) solid line-exact, eqn.(11); b) dashed line-errorless data predictions, $\epsilon_2 = 0$, eqn.(2d); and c) open triangle-noisy data predictions, $\epsilon_2 = 0.1$, eqn.(2d) when $M = 3000$.

$$\|\epsilon_{OUT}(q_s'')\|_2 = \sqrt{\frac{\sum_{i=1}^{M}(q_s''(t_i) - q_{s,i}'')^2}{M}}, \tag{13}$$

where $q_{s,i}''$, $i = 1, 2, ..., M$ are the numerically obtained values for the heat flux. Equation (13) also notationally contains the data source used for estimating the heat flux. The RMS input data error tends to be relatively constant over M for fixed error, ϵ_i, $i = 1, 2$. This is in line with physical expectations associated with random errors and is thus not numerically detailed. Figure 6 displays the behavior of the root-mean-square (RMS) of the output error (W/m^2) as the sample density is increased for two induced noise levels for both data types. Figure 6 displays the RMS output error results for $\epsilon_1 = 0.0125$ (open circle), $\epsilon_1 = 0.025$ (filled circle), and $\epsilon_2 = 0.1$ (open triangle), $\epsilon_2 = 0.2$ (filled triangle) as the sample density M is increased. The heating/cooling rate data clearly presents a favorable trend for the accurate and reliable prediction of the surface heat flux. That is, error reduction is observed when applying heating/cooling rate data while error amplication is observed when applying the temperature data.

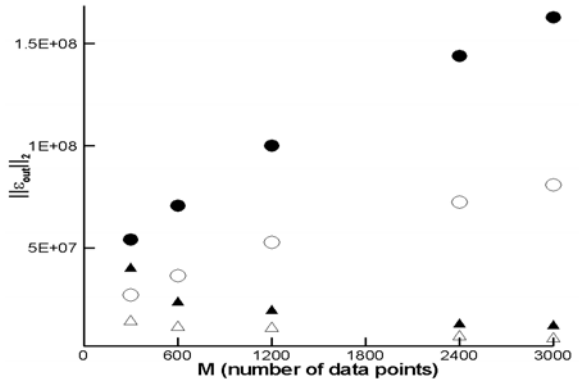

Figure 6: Root-mean-square of the output error (W/m^2), eqn.(13) over sample density (temperature data: open circle - $\epsilon_1 = 0.0125$, filled circle - $\epsilon_1 = 0.025$; and heating/cooling rate data: open triangle - $\epsilon_2 = 0.1$, filled triangle - $\epsilon_2 = 0.2$).

4. CONCLUSIONS

This paper conveys the need and benefit for the direct measurement or interpretation of a higher-time derivative of temperature for real-time applications. Accurate standalone sensors do not guarantee accurate predictions of other quantities unless a clear understanding of how the data propagates through the mathematical formulation. Frankel and his colleagues are presently developing sensor concepts for the direct measurement of heating/cooling rate, dT/dt.

REFERENCES

1. F.K. Lu, and D.E. Marren, eds., *Advanced Hypersonic Test Facilities*, Progress in Astronautics and Aeronautics, Vol.**198**, VA, 2002.

2. R. Kress, *Linear Integral Equations*, Springer-Verlag, Berlin, 1989.

3. T. Groetsch, Differentiation of approximately specified functions. *Amer. Math. Month.* (1991) **98**, 847-850.

4. G.M. Wing, *A Primer on Integral Equations of the First Kind*, SIAM, Philadelphia, PA, 1991.

5. J.I. Frankel, G.E. Osborne and K. Taira, Stabilization of ill-posed problems through the data space. *AIAA J. Thermophys. Heat Transfer*, (to appear).

6. V.V. Kulish and J.L. Lage, Fractional diffusion solutions for transient local temperature and heat flux. *J. Heat Transfer* (2000) **122** (2), 372-376.

7. C.A. Brebbia, J.C.F. Telles and L.C. Wrobel, *Boundary Element Techniques*, Springer-Verlag, NY, 1984.

8. P. Linz, *Analytical and Numerical Methods for Volterra Equations*, SIAM, Philadelphia, PA, 1985.

9. M. Abramowitz and I.A. Stegun, *Handbook of Mathematical Functions*, Dover, NY, 1972.

10. J.I. Frankel and J.J. Lawless, Numerically stabilizing ill-posed moving surface problems through heat rate sensors. *AIAA J. Thermophys. Heat Transfer*, (to appear).